Further Insights into Quinone Cofactor Biogenesis: Probing the Role of *mauG* in Methylamine Dehydrogenase Tryptophan Tryptophylquinone Formation†

Arwen R. Pearson,‡,⊥ Teresa De la Mora-Rey,‡,⊥ M. Elizabeth Graichen,§,⊥ Yongting Wang,§ Limei H. Jones,§ Sudha Marimanikkupam,‡ Sean A. Agger,‡ Paul A. Grimsrud,‡ Victor L. Davidson,§ and Carrie M. Wilmot*,‡

Department of Biochemistry, Molecular Biology and Biophysics, University of Minnesota, Minneapolis, Minnesota 55455, and Department of Biochemistry, The University of Mississippi Medical Center, Jackson, Mississippi 39216

Received January 16, 2004; Revised Manuscript Received March 3, 2004

ABSTRACT: *Paracoccus denitrificans* methylamine dehydrogenase (MADH) is an enzyme containing a quinone cofactor tryptophan tryptophylquinone (TTQ) derived from two tryptophan residues (βTrp^{57} and βTrp^{108}) within the polypeptide chain. During cofactor formation, the two tryptophan residues become covalently linked, and two carbonyl oxygens are added to the indole ring of βTrp^{57}. Expression of active MADH from *P. denitrificans* requires four other genes in addition to those that encode the polypeptides of the MADH $\alpha_2\beta_2$ heterotetramer. One of these, *mauG*, has been shown to be involved in TTQ biogenesis. It contains two covalently attached *c*-type hemes but exhibits unusual properties compared to *c*-type cytochromes and diheme cytochrome *c* peroxidases, to which it has some sequence similarity. To test the role that MauG may play in TTQ maturation, the predicted proximal histidine to each heme (His^{35} and His^{205}) has each been mutated to valine, and wild-type MADH was expressed in the background of these two *mauG* mutants. The resultant MADH has been characterized by mass spectrometry and electrophoretic and kinetic analyses. The majority species is a TTQ biogenesis intermediate containing a monohydroxylated βTrp^{57}, suggesting that this is the natural substrate for MauG. Previous work has shown that MADH mutated at the βTrp^{108} position (the non-oxygenated TTQ partner) is predominantly also this intermediate, and work on these mutants is extended and compared to the MADH expressed in the background of the histidine to valine *mauG* mutations. In this study, it is unequivocally demonstrated that MauG is required to initiate the formation of the TTQ cross-link, the conversion of a single hydroxyl located on βTrp^{57} to a carbonyl, and the incorporation of the second oxygen into the TTQ ring to complete TTQ biogenesis. The properties of MauG, which are atypical of *c*-type cytochromes, are discussed in the context of these final stages of TTQ biogenesis.

Methylamine dehydrogenase (MADH)[1] from *Paracoccus denitrificans* is a periplasmic $\alpha_2\beta_2$ heterotetrameric enzyme responsible for the conversion of methylamine to formaldehyde and ammonia (*1*, *2*). The oxidative deamination of methylamine also produces two electrons that are fed into the oxidative metabolic pathway of *P. denitrificans* via specific electron-transfer proteins, amicyanin (*3*), and cytochromes *c*-551i and *c*-550 (*4*, *5*). MADH is one of a growing number of enzymes that have been shown to contain protein-derived posttranslationally modified cofactors. The existence of protein-derived cofactors has been demonstrated relatively recently, so their abundance and diversity is only just coming to light (*6*, *7*). In their simplest form biogenesis is self-processing, as is seen with topaquinone (TPQ) in amine oxidases. This may represent an evolutionary pathway that enabled proteins to harness organic chemistries that were beyond the capabilities of the 20 amino acids without the need for an exogenously synthesized cofactor (*8*−*10*). However, similar cofactors have evolved that require other enzymes for biogenesis, as is the case for the more complex tryptophan tryptophylquinone (TTQ) of MADH, which is derived from two β subunit tryptophan residues (*11*). To generate the TTQ cofactor of MADH from *P. denitrificans*, two oxygens are incorporated into the indole ring of βTrp^{57} and a covalent bond is formed between the indole rings of βTrp^{57} and βTrp^{108} (Figure 1).

In previous work, site-directed mutagenesis was used to convert βTrp^{108} to a histidine or cysteine. The results of that study demonstrated that incorporation of the two quinone oxygens into TTQ is a two step process involving discrete monoxygenase reactions (*12*). The incorporation of the second oxygen appeared to be highly coupled to formation of the covalent cross-link between βTrp^{57} and βTrp^{108}. Mutation of βTrp^{108} to histidine or cysteine resulted in a majority expressed species of MADH β subunit into which

† This work was supported by NIH Grants GM-66569 (C.M.W.) and GM-41574 (V.L.D.).

* To whom correspondence should be addressed. Tel: 612-624-2406. Fax: 612-624-5121. E-mail: wilmo004@umn.edu.

‡ University of Minnesota.

§ The University of Mississippi Medical Center.

⊥ These authors contributed equally to the work.

[1] Abbreviations: MADH, methylamine dehydrogenase; TTQ, tryptophan tryptophylquinone; TPQ, topaquinone; CTQ, cysteine tryptophylquinone; HTQ, histidine tryptophylquinone; wtMADH, recombinantly expressed wild-type methylamine dehydrogenase; H35V/MADH and H205V/MADH, wild-type MADH expressed in cells with H35V or H205V mutations, respectively, in *mauG*; DCIP, 2,6-dichlorophenolindophenol; DTT, dithiothreitol; TFA, trifluoroacetic acid; MALDI, matrix-assisted laser desorption ionization; TOF, time-of-flight; ESI, electrospray ionization; QTOF, quadrupole time-of-flight.

10.1021/bi049863l CCC: $27.50
Published on Web 04/13/2004

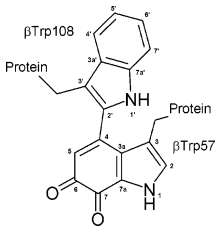

FIGURE 1: Structure of tryptophan tryptophylquinone (TTQ).

only a single oxygen had been posttranslationally incorporated. The MADH mutants with incompletely biosynthesized cofactor also exhibited weakened α/β subunit interactions (*12*). A small percentage of the enzyme in each βW108H and βW108C preparation appeared to contain a mature (H/C)TQ cofactor, which probably accounted for the small amount of activity observed in each preparation.

MADH is located within the methylamine utilization (*mau*) gene cluster of *P. denitrificans*, which is induced in response to growth on methylamine as a sole carbon source (*13*). The cluster encodes the two α (*mauB*) and β (*mauA*) subunits of MADH and its specific electron acceptor, amicyanin (*mauC*), as well as eight other genes (*1*). Four genes, *mauD*, *E*, *F*, and *G*, have been shown to be required for the biosynthesis of MADH and its cofactor. Unmarked deletion mutations in *mauD*, *E*, or *F* each resulted in undetectable levels of β subunit (*1, 14, 15*). The gene products of *mauD*, *E*, and *F* have never been isolated, so their putative functions have been inferred from their sequences. The deduced sequence of *mauD* contains a CXXC motif associated with disulfide bond formation and may therefore be involved in the processing of the six disulfide bonds that are present in the MADH β subunit (*15*). The *mauE* product appears to be an integral membrane protein and has been proposed to be a possible β subunit transporter (*15*). No function has been assigned to the *mauF* product, which has no obvious sequence homology to any known proteins. In contrast to the *mauD*, *E*, and *F* deletions, in the *mauG* deletion mutant strain, the MADH β subunit was synthesized and translocated to the periplasm at near wild-type levels (*1*). However, no MADH activity was observed. This suggested a specific role for MauG in posttranslational processing of MADH and possibly TTQ biogenesis. The sequence of *mauG* encodes two heme *c* binding motifs (CXXCH) and shows homology to the diheme cytochrome *c* peroxidases (*1*). The MauG protein has recently been expressed and characterized (*16*). It does possess two covalently bound hemes but exhibits only very weak peroxidase activity. It also has an electron paramagnetic resonance (EPR) spectrum and characteristics, such as carbon monoxide and oxygen binding, more akin to oxygen-binding heme proteins. These results suggested a potentially novel activity for one or both of the *c*-type hemes of MauG that could enable it to catalyze oxygen incorporation, as well as cross-link formation, during the biogenesis of TTQ.

In this study, the role of MauG in MADH and TTQ biogenesis was probed by using site-directed mutagenesis to individually alter each of the proximal histidine ligands predicted from the CXXCH heme *c* binding motifs of MauG. MADH was expressed in a heterologous expression system (*17*) from a plasmid that contains the structural genes for MADH, the mutated *mauG* sequences, and the additional *mau* genes that are required for MADH biosynthesis. The MADH β subunit expressed in the background of these mutations in *mauG* was characterized to determine the extent to which the posttranslational modifications in the biogenesis of TTQ had occurred. The MADH β subunits of the previously described βW108H and βW108C mutants of MADH (*12*) have also been more thoroughly analyzed to determine the presence or absence of a cross-link with residue βTrp^{57} and confirm the residue into which oxygen was posttranslationally incorporated. These results provide new insight into the mechanisms of TTQ biogenesis and of posttranslational modification and oxygenation of amino acid residues in proteins.

Table 1: Bacterial Strains and Plasmids

strain or plasmid	relevant features	source or reference
	Bacteria	
E. coli JM109	general cloning strain	Promega
E. coli S17-1	conjugative donor, *mob*$^+$ Sm^r	ref *23*
R. sphaeroides 2.4.1	wild-type	laboratory strain
	Plasmids	
pMEG993	pBSII SK, *mauFBEDACJG*	ref *17*
pMEG976	pRK415-1, *coxII* pr, *mauFBEDA*−*6-hisCJG*	ref *18*
pMEG423	pRK415-1, *coxII* pr, *mauFBEDA*−*6-hisCJG*(H35V)	this work
pMEG424	pRK415-1, *coxII* pr, *mauFBEDA*−*6-hisCJG*(H205V)	this work

EXPERIMENTAL PROCEDURES

Protein Purification. Recombinant polyhistidine-tagged *P. denitrificans* MADH was heterologously expressed in *Rhodobacter sphaeroides* as described previously (*17, 18*). Proteins were purified using a Ni^{2+}-NTA superflow column (Qiagen) from either sonicated whole cell extracts or periplasmic cell fractions by previously described procedures (*18*).

Molecular Biology. The bacterial strains and plasmids used in this study are shown in Table 1. A 1.4 kb section from pMEG993 containing the *mauG* gene was excised with *Pst*I and *Apa*I and ligated into the multiple cloning region of pBluescript^R II SK (Stratagene) to create a small plasmid for ease of mutagenesis. The H35V and H205V mutations were created using this template with the QuikChange site-directed mutagenesis kit (Stratagene). The primers used to create the mutations were: 5′-CCTGCGCCACCTGTGTC-GACCCCGCCCGC-3′ for H35V and 5′-CCTGGAACTGC-CGGCTCTGCGTCATGCAGCG-3′ for H205V. For each, the complementary sequence was used as the second primer for the mutagenesis. The underlined bases are those that were changed to create the desired mutation, as well as additional changes that were incorporated to generate or remove a restriction site to facilitate screening for the mutation. Mutations were confirmed by sequencing, and *Pst*I to *Apa*I sections containing the H35V or H205V mutations were excised from the mutation plasmids and ligated into the *mau* gene cluster in place of the original *Pst*I to *Apa*I section in pMEG976 (*18*), which already contains a hexahistidine tag at the C-terminal end of the β subunit of MADH and the *coxII* promoter (Table 1). The 6.9 kb *coxII* promoter−*mauFBEDA*−*6-hisCJG* sections were then excised with *Kpn*I and inserted into the broad-host-range vector pRK415-1 (*19*),

which had been opened with *Kpn*I and phosphatase-treated, to form pMEG423 and pMEG424, containing the *mauG*-(H35V) and *mauG*(H205V) mutations, respectively. These plasmids were introduced into *R. sphaeroides* 2.4.1 cells via conjugation through *E. coli* S17-1 cells (*17*).

Kinetic Assay. Steady-state kinetic assays of MADH were performed with artificial electron acceptors as described previously (*20*) in 0.1 M potassium phosphate, pH 7.5, at 30 °C. The standard assay mixture contained 16 nM MADH, varied concentrations of methylamine, 4.8 mM phenazine ethosulfate, and 170 μM 2,6-dichlorophenolindophenol (DCIP). The reaction was monitored at 600 nm to determine the rate of reduction of DCIP. When assaying sample for MADH activity, a saturating concentration (10 mM) of methylamine was present.

Electrophoretic Techniques. Samples containing recombinant wild-type MADH (wtMADH), βW108H mutant MADH, and wtMADH expressed with either H35V (H35V/MADH) or H205V (H205V/MADH) mutations in *mauG* were subjected to SDS−polyacrylamide gel electrophoresis (SDS−PAGE), using a 4−12% gradient gel, and nondenaturing PAGE using a 4−20% gradient gel. Gels were stained for protein with Coomassie Blue G250. The nondenaturing gels were also stained for MADH activity by incubation overnight in a solution of 0.5 M potassium phosphate, pH 7.5, which contained an excess of methylamine and nitroblue tetrazolium.

Proteolysis of Wild Type, Mutant, and Incompletely Biosynthesized MADH. Prior to proteolytic digest, samples were derivatized to block the potentially reactive quinone of TTQ, if present, as well as the free sulfhydryls present in MADH following disulfide reduction. MADH samples (7−14 μM) were incubated with 75 μM hydroxylamine at room temperature for 10 min to covalently modify any quinone present so that it would not react with protein amine groups when denatured (*21*). Guanidine-HCl was then added to a final concentration of 3.6 M, and the mixture was incubated at 37 °C for 30 min. Disulfide bonds were reduced by addition of 45 mM dithiothreitol (DTT) and incubation at room temperature for 20 min. The free cysteines were protected from reoxidation by the addition of 65 mM iodoacetamide and incubation in the dark at room temperature for 20 min. A further addition of 120 mM DTT and incubation at room temperature for 5 min followed. Aliquots of sample were assayed by MALDI-TOF mass spectrometry to check that derivatization was complete.

After derivatization, proteolysis was performed using either trypsin or chymotrypsin. Samples were diluted by addition of 100 mM ammonium bicarbonate (pH 8.5−9) so that the final concentration of guanidine-HCl was 1.5 M and then incubated with 0.1 mg/mL protease. The resulting mixture was divided into two, and one-half was left for 2 h and the other overnight at room temperature. Controls for proteolytic self-cleavage were prepared by incubating each protease at the same concentration under the same conditions as the experimental samples. Aliquots of each digestion were subjected to MALDI-TOF mass spectrometry to check that proteolysis was complete by confirming the absence of any high molecular weight peaks.

MALDI-TOF Mass Spectrometry. Since the MADH peptides of interest varied in size, proteolyzed MADH samples were desalted using either C18 or C4 zip tips. In brief, zip tips were hydrated by washing twice with 50% acetonitrile and 0.1% trifluoroacetic acid (TFA) in water, then washing twice with 0.1% TFA in water. The sample was loaded and washed six times in 5% acetonitrile and 0.1% TFA and eluted from C18 or C4 zip tips with 1.2 μL of 60% acetonitrile and 0.1% TFA or 1.5 μL of 70% acetonitrile and 0.1% TFA, respectively. One microliter of α-cyano-4-hydroxycinnamic acid (CCA) matrix or sinapinic acid (SA) matrix was added to the samples eluted in 60% acetonitrile or 70% acetonitrile, respectively. One microliter of these mixtures was placed on a MALDI-TOF target and allowed to dry. Mass spectra were acquired on a Biflex MALDI-TOF mass spectrometer (Bruker Daltonics) equipped with a N_2 laser. Larger peptides were analyzed with the help of linear mode and smaller peptides using reflectron mode. Calibration was performed using cytochrome *c* (monoisotopic mass [MH^+] 12 361.088 Da), angiotensin I (monoisotopic mass [MH^+] 1296.685 Da), and angiotensin II (monoisotopic mass [MH^+] 1046.542), which were obtained from Sigma-Aldrich, St. Louis, MO.

ESI Mass Spectrometry. Whole and proteolyzed MADH samples for ESI mass spectral analysis were desalted using 20 μm Porus R2 resin (ABI, polystyrene divinylbenzene) in a glass purification capillary. Whole protein samples were loaded onto the R2 resin, washed three times with ~5 μL of 5% methanol, 0.5% formic acid and eluted with ~2.5 μL of 70% methanol, 0.5% formic acid into a coated nanoelectrospray capillary (Protana Engineering, Denmark). Proteolyzed samples were diluted with acetonitrile instead of methanol.

ESI mass spectra were acquired using a QSTAR Pulsar *i* (Applied Biosystems, Inc. (ABI), Foster City, CA) quadrupole-TOF (time-of-flight) mass spectrometer equipped with a nano-ESI source (Protana Engineering, Denmark). The ion spray voltage was 1000 V, the TOF region acceleration voltage was 4 kV, and the injection pulse repetition rate was 7.0 kHz. External calibration was performed using renin (monoisotopic mass [MH^{3+}] 586.9830 and [MH^{2+}] 879.9705; Sigma-Aldrich, St. Louis, MO). Mass spectra were the average of approximately 300 scans collected in positive mode over a 5 min acquisition period. MS/MS fragmentation and *m*/*z* measurements from the proteolyzed samples were carried out on peptides of interest with an injection pulse repetition rate of 5.0 kHz using nitrogen as the collision gas. MS/MS analysis was carried out using the automated sequencing algorithm of the Bioanalyst, AnalystQS software package (ABI). The tolerance for defining a peak match in the fragmentation was set at a *m*/*z* of ±150 ppm. All ions with intensity greater than 7% have been accounted for in the MS/MS spectra.

RESULTS

Extracts of *R. sphaeroides* cells expressing recombinant MADH encoded by plasmids pMEG976, pMEG423, and pMEG424 (Table 1) were prepared by either ultrasonic disruption or periplasmic fractionation (*22*). Each extract was applied to a Ni^{2+}-NTA superflow column (Qiagen) and then eluted with buffer that contained increasing concentrations of imidazole. The 6×His-MADH eluted at approximately 50 mM imidazole. The proteins isolated from pMEG423 and pMEG424 are designated, respectively, H35V/MADH and H205V/MADH. In contrast to wtMADH, the fractions containing H35V/MADH and H205V/MADH exhibited

relatively low activity and no clearly discernible visible absorption spectrum. These altered forms of MADH were characterized by steady-state kinetics, electrophoresis, and mass spectrometry.

Kinetic Analysis. H35V/MADH and H205V/MADH were analyzed by steady-state kinetics using artificial electron acceptors. Since the protein expressed in the background of the *mauG* mutations lacks the characteristic spectral features of TTQ, the exact concentration could not be determined from the extinction coefficient of the cofactor, as is done with native MADH. Instead, the concentrations of H35V/MADH and H205V/MADH were estimated from the absorption of the protein at 280 nm and by comparison with samples of known concentration of MADH after SDS−PAGE and staining for protein. The activity of preparations varied from batch to batch from undetectable levels to k_{cat} values of 2.9 s^{-1}, compared to 32 s^{-1} for wtMADH (*17*). The majority of the preparations of both H35V/MADH and H205V/MADH exhibited k_{cat} values of <1 s^{-1}. K_m values for methylamine for H35V/MADH and H205V/MADH with detectable activities each averaged about 25 μM, compared to that of wtMADH of 8 μM (*17*). The steady-state assay yields very reproducible results, and as discussed below, the observed activity could be attributed to a small subpopulation that appears to possess correctly processed TTQ. Since k_{cat} values are determined using the total amount of protein present, the variability in k_{cat} reflects variability in the proportion of this subpopulation in different preparations. To show that the activity of H35V/MADH and H205V/MADH could be attributed to the reactivity of a carbonyl-containing cofactor, the samples were pretreated with phenylhydrazine, which forms a covalent adduct with TTQ in native MADH (*21*). Samples were incubated for 20 min with a 10-fold molar excess of phenylhydrazine and then dialyzed to remove the unreacted reagent. This treatment eliminated essentially all of the observed activity in the wtMADH, H35V/MADH, and H205V/MADH.

Electrophoretic Analysis. H35V/MADH and H205V/MADH were analyzed by SDS−PAGE and nondenaturing PAGE and compared with recombinant wtMADH. For comparison and later discussion, the βW108H MADH mutant (*12*) was also included in these analyses. Analysis by SDS−PAGE revealed that the α and β subunits of MADH were present in both H35V/MADH and H205V/MADH and are correctly processed with respect to overall polypeptide size (Figure 2A). The additional minor bands are endogenous *R. sphaeroides* proteins that bind to the affinity column. While these contaminants can be removed by further purification, this also resulted in significant loss of βW108H MADH, H35V/MADH, and H205V/MADH, due to their relative instability compared to wtMADH. Thus, samples isolated directly from cell extracts with the affinity column were compared.

In contrast with the results of the SDS−PAGE analysis, the analysis of the proteins by nondenaturing PAGE revealed significant differences between the wtMADH and the H35V/MADH and H205V/MADH preparations. The wtMADH migrates as a single band, corresponding to the $\alpha_2\beta_2$ heterotetramer. H35V/MADH and H205V/MADH migrate primarily as two bands, which correspond to the positions of migration of the isolated α and β subunits of wtMADH (Figure 2B). A small amount of each sample, however, migrates to a position corresponding to that of the wtMADH $\alpha_2\beta_2$ heterotetramer. For all MADH samples, an activity stain of the gel showed that only the $\alpha_2\beta_2$ heterotetramer band had positive activity (Figure 2C). This pattern has also been observed for the MADH mutants βW108H (Figure 2B) and βW108C (*12*). The activity staining technique is very sensitive but qualitative because it is difficult to establish a linear range at the higher levels of activity since the gel is allowed to incubate with the reaction mixture for an extended time to observe weak reactivity. A qualitative correlation, however, is always seen between the level of protein stain and activity stain of the $\alpha_2\beta_2$ heterotetramer band, and no activity is ever observed from either the α or β subunit bands. The level of protein and activity stain of the $\alpha_2\beta_2$ heterotetramer band also correlates with the k_{cat} value observed for the enzyme in solution (discussed earlier) and also with the relative intensity of the peak in the mass spectrum corresponding to fully biosynthesized β subunit (discussed later).

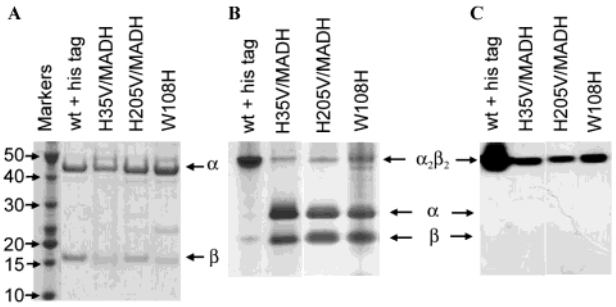

FIGURE 2: Electrophoretic analysis of recombinant wtMADH, MADH mutant βW108H, and wild-type MADH expressed in the background of the *mauG* mutations H35V (H35V/MADH) and H205V (H205V/MADH). The positions that correspond to those of the purified α and β subunits and the $\alpha_2\beta_2$ holoenzyme are indicated. All samples have an N-terminal 6×His-tag and were expressed in *Rhodobacter sphaeroides*: (A) SDS−PAGE stained for protein; (B) native nondenaturing PAGE stained for protein; (C) native nondenaturing PAGE stained for methylamine dehydrogenase activity.

Whole Protein Mass Spectrometry of H35V/MADH and H205V/MADH. MADH samples were analyzed by ESI mass spectrometry. These results are summarized in Table 2. The theoretical mass for the fully biosynthesized β subunit was calculated from the amino acid sequence, taking into account formation of six disulfide bonds, a cross-link between βTrp^{57} and βTrp^{108}, and the incorporation of two carbonyl oxygens into βTrp^{57}. Wild-type MADH showed a single mass for the β subunit corresponding to a β subunit containing a fully synthesized TTQ (Figure 3A). Both H35V/MADH and H205V/MADH showed a major peak corresponding to a β subunit containing the six disulfides and a single extra oxygen (Figure 3B and C). In addition to the major peak, both samples also showed two minor peaks. The larger was at a mass corresponding to a β subunit with fully synthesized TTQ. The second very minor peak was at a mass corresponding to a β subunit with six disulfides and no additional oxygens. No other posttranslational modifications were observed for either H35V/MADH or H205V/MADH.

Proteolysis and Mass Spectrometry of H35V/MADH and H205V/MADH. Proteolysis of samples was performed to determine definitively whether the covalent cross-link between βTrp^{57} and βTrp^{108} was absent or present and to define the position and form of the additional oxygen that was incor-

Table 2: Assignment of Peaks from Mass Spectral Analysis

modification	calcd mass (Da)[a]	obsd mass (Da)[b] H35V/MADH	H205V/MADH	wtMADH
formation of six disulfide bonds, no additional oxygen	14 981.5	14 980.1 ± 2.0	14 981.9 ± 0.9	*c*
formation of six disulfide bonds, incorporation of one hydroxyl	14 997.5	14 996.8 ± 0.4	14 997.1 ± 0.3	*c*
fully biosynthesized	15 009.5	15 010.9 ± 0.5	15 011.1 ± 0.4	15 009.3 ± 0.1

[a] Theoretical masses were calculated using GPMAW 5.02b (Lighthouse data, Denmark). Wild-type and mutant subunits each possess a 6×His tag at the C-terminus. Fully biosynthesized subunits possess six intrasubunit disulfide bonds, two quinone carbonyl oxygens, and a covalent cross-link between tryptophan residues as described in the text. [b] Errors in observed mass were calculated using the following equation: $\sqrt{\Sigma(zE_z)^2 I_z/\Sigma I_z} = {}^1/_2 E_{\text{overall}}$, where z is the charge species, E_z is the error in measurement of charge species z, and I_z is the intensity of the charge species. E_z, z, and I_z are output by the deconvolution software for each peak used in protein zero mass determination. [c] Not present.

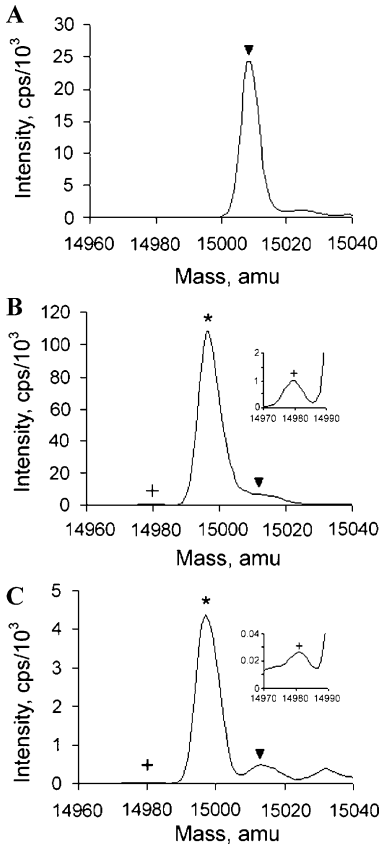

FIGURE 3: Deconvoluted mass spectra of (A) recombinant wt-MADH, (B) H35V/MADH, and (C) H205V/MADH. All samples have a C-terminal 6×His-tag. Deconvolution was performed with the following parameters: mass range to search for deconvoluted peaks was 14 000−16 000 Da; other parameters were left at the software default values (Bayesian Protein Reconstruct tool in the ABI BioAnalyst software package). Symbols are as follows: "+" corresponds to a β-subunit mass with six disulfides (insets in panels B and C show a magnification of this area of the spectrum), "∗" corresponds to a β-subunit mass with six disulfides, no cross-link, and incorporation of one oxygen atom, and "▼" corresponds to a β-subunit mass with six disulfides and a fully synthesized TTQ cofactor.

porated into H35V/MADH and H205V/MADH. Trypsin and chymotrypsin each have predicted cleavage sites located in the sequence between βTrp^{57} and βTrp^{108}. If a cross-link was present, then the resulting two peptides containing βTrp^{57} and βTrp^{108} would remain covalently linked, giving a combined mass. If there was no cross-link present then the two peptides would show up in the mass spectrum as individual distinct species.

For H35V/MADH, the trypsin digestion gave a *m*/*z* peak of 908.43 amu, which corresponded to the +3 charge state of the predicted trypsin cleavage product of the residues βLeu^{52}−βArg^{75} with a single additional oxygen. MS/MS fragmentation was performed to sequence the peptide (Figure 4A). The carboxamidomethyl modification to βCys^{61} was taken into account, and only when a hydroxyl group was added to the mass of βTrp^{57} in place of a hydrogen did the b6, b7, b8, and b12 product ion masses (different length fragments that include the N-terminus of the peptide, Figure 4A) match the *m*/*z* peaks observed in the mass spectrum. This definitively demonstrated that the additional oxygen in the majority species of the H35V/MADH was present on βTrp^{57} and was in the form of a hydroxyl and that this peptide was not cross-linked to βTrp^{108}. The chymotrypsin digest of H35V/MADH gave a *m*/*z* peak of 1102.86 amu, which corresponded to the +3 charge state of the predicted chymotrypsin cleavage product of the residues βAsn^{81}−βTrp^{108}. Sequencing by MS/MS fragmentation of this peak confirmed that it was the βTrp^{108}-containing peptide (Figure 4B). The presence of the βTrp^{108}-containing peptide again confirmed the absence of the cross-link in the majority species observed in the H35V/MADH sample.

In the chymotrypsin digest of H205V/MADH, the *m*/*z* peak corresponding to the un-cross-linked βAsn^{81}−βTrp^{108} peak was present, and its sequence was confirmed by MS/MS fragmentation (Figure 5B). In addition, a *m*/*z* peak of 1136.83 amu was present that corresponded to the predicted chymotrypsin cleavage product βArg^{27}−βTrp^{57}, containing βTrp^{57}, with a charge of +3. This 31 amino acid peptide is large for MS/MS fragmentation sequence analysis, but nevertheless a good fit to the sequence was obtained (Figure 5A). As with H35V/MADH, only when a hydroxyl group was added to the mass of βTrp^{57} in place of a hydrogen for H205V/MADH did y product ions (y1, y2, y4, y9, y10, and y11, different length fragments that include the C-terminus of the peptide, Figure 5A) match the *m*/*z* peaks in the mass spectrum.

Thus, the majority species of H35V/MADH and H205V/MADH each contains no cross-link between βTrp^{57} and βTrp^{108} and has one oxygen incorporated into residue βTrp^{57} in the form of a hydroxyl.

Proteolysis and Mass Spectrometry of βW108H and βW108C MADH. It was previously demonstrated by whole protein mass spectrometry that the majority species of βW108H and βW108C MADH mutants each possessed only one posttranslationally incorporated oxygen in the β subunit (*12*). Further analysis was not possible because the protocol

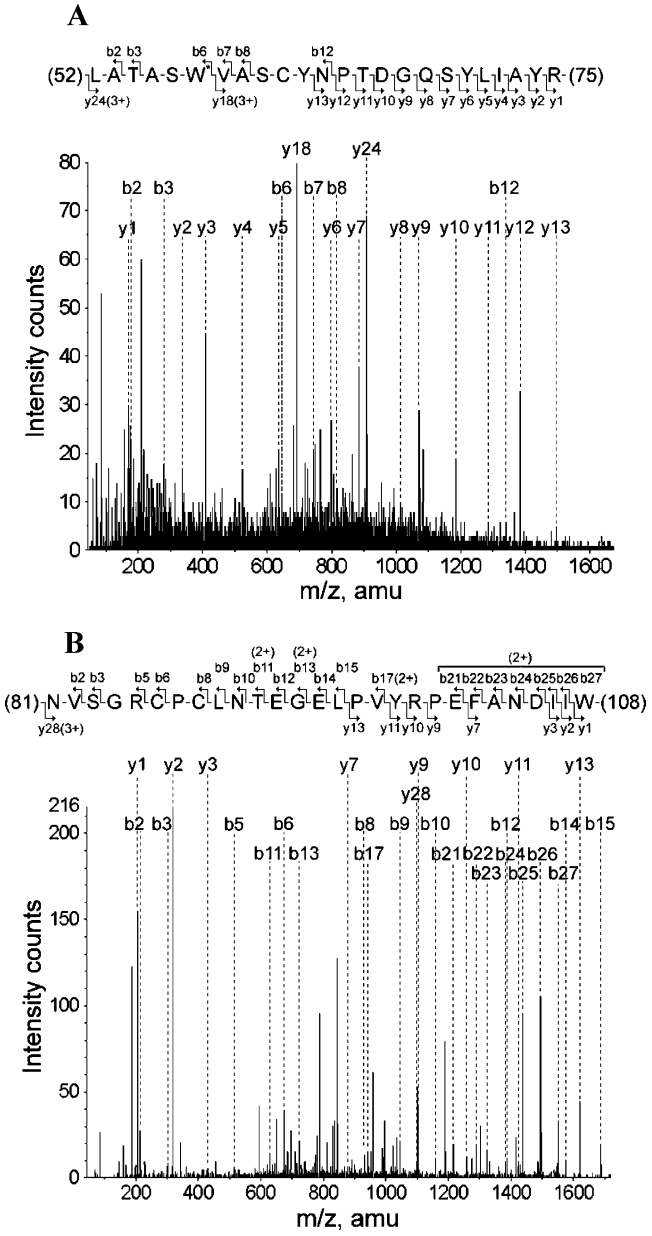

FIGURE 4: MS/MS spectra from fragmented proteolyzed peptides of H35V/MADH obtained by ESI-QTOF. Cysteine residues were protected from oxidation, and their masses include the addition of carboxamidomethyl. Product ions that were observed in the spectrum only as a multicharged species have the charge indicated in parentheses. Tolerance for *m*/*z* peak matches with product ions was set at ±150 ppm, and only b and y ions with intensities greater than 2% have been reported. Panel A shows the MS/MS spectrum of the triply charged ion of peptide βLeu^{52}−βArg^{75} at *m*/*z* 908.43 generated by trypsin cleavage. The position of βTrp^{57}, the residue that becomes the quinone, is indicated by W* in the sequence. The *m*/*z* peaks for product ions b6, b7, b8, b12, and y24 only matched the spectrum when a hydroxyl was added to the mass of βTrp^{57} in place of a hydrogen. Panel B shows the MS/MS spectrum of the triply charged ion of peptide βAsn^{81}−βTrp^{108} at *m*/*z* 1102.86 generated by chymotrypsin cleavage. The residue βTrp^{108} becomes covalently cross-linked to βTrp^{57} in the final TTQ cofactor.

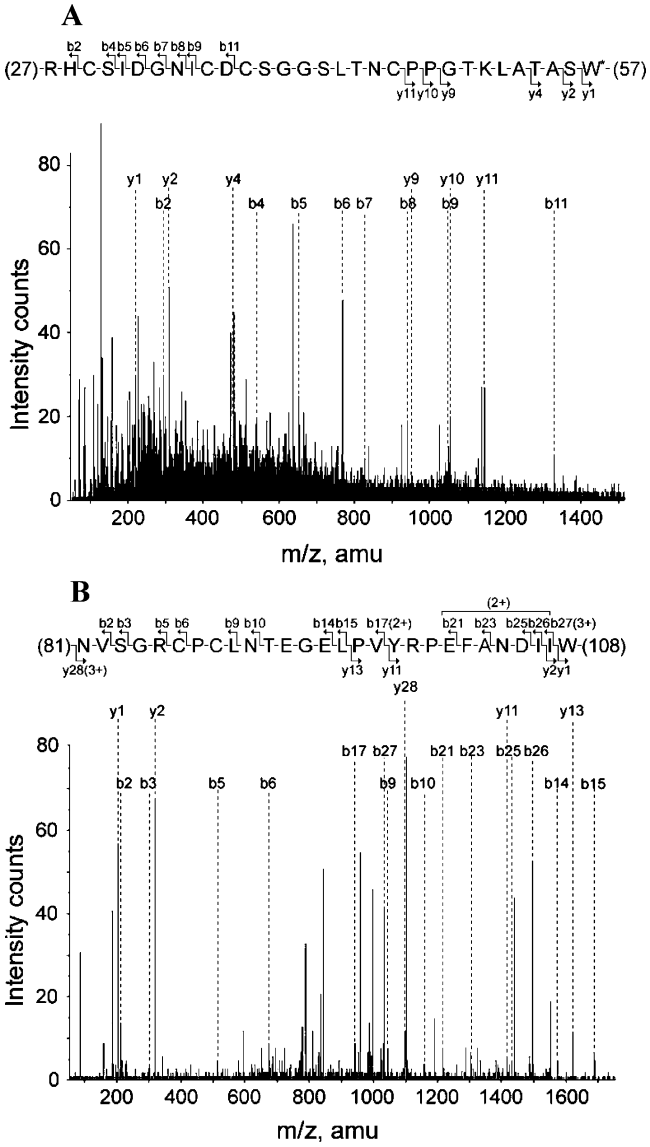

FIGURE 5: MS/MS spectra from fragmented proteolyzed peptides of H205V/MADH obtained by ESI-QTOF. Cysteine residues were protected from oxidation, and their masses include the addition of carboxamidomethyl. Product ions that were observed in the spectrum only as a multicharged species have the charge indicated in parentheses. Tolerance for *m*/*z* peak matches with product ions was set at ±150 ppm, and only b and y ions with intensities greater than 2% have been reported. Panel A shows the MS/MS spectrum of the triply charged ion of peptide βArg^{27}−βTrp^{57} at *m*/*z* 1136.83 generated by chymotrypsin cleavage. The position of βTrp^{57}, the residue that becomes the quinone, is indicated by W* in the sequence. The *m*/*z* peaks for product ions y1, y2, y4, y9, y10, and y11 only matched the spectrum when a hydroxyl was added to the mass of βTrp^{57} in place of a hydrogen. Panel B shows the MS/MS spectrum of the triply charged ion of peptide βAsn^{81}−βTrp^{108} at *m*/*z* 1102.86 generated by chymotrypsin cleavage. The residue βTrp^{108} becomes covalently cross-linked to βTrp^{57} in the final TTQ cofactor.

for proteolytic digestion of the β subunit had not been established at that time. The MADH β-subunit is difficult to unfold because it has six intrasubunit disulfide bonds, as well as the covalent TTQ cross-link, when present. Neither boiling nor treatment with 6 M urea unfolds either the wild-type or mutant MADH β subunits enough to allow full reduction of disulfides and their protection by iodoacetamide, as assessed by MALDI-TOF mass spectral analysis. Only prolonged incubation with 3.5 M guanidine-HCl enabled the protein to be unfolded enough for disulfide reduction. Even after protection of the free cysteines, removal of the guanidine-HCl led to partial refolding limiting access to cleavage sites for the proteases. Finally it was found that the proteases could function in milder denaturing conditions

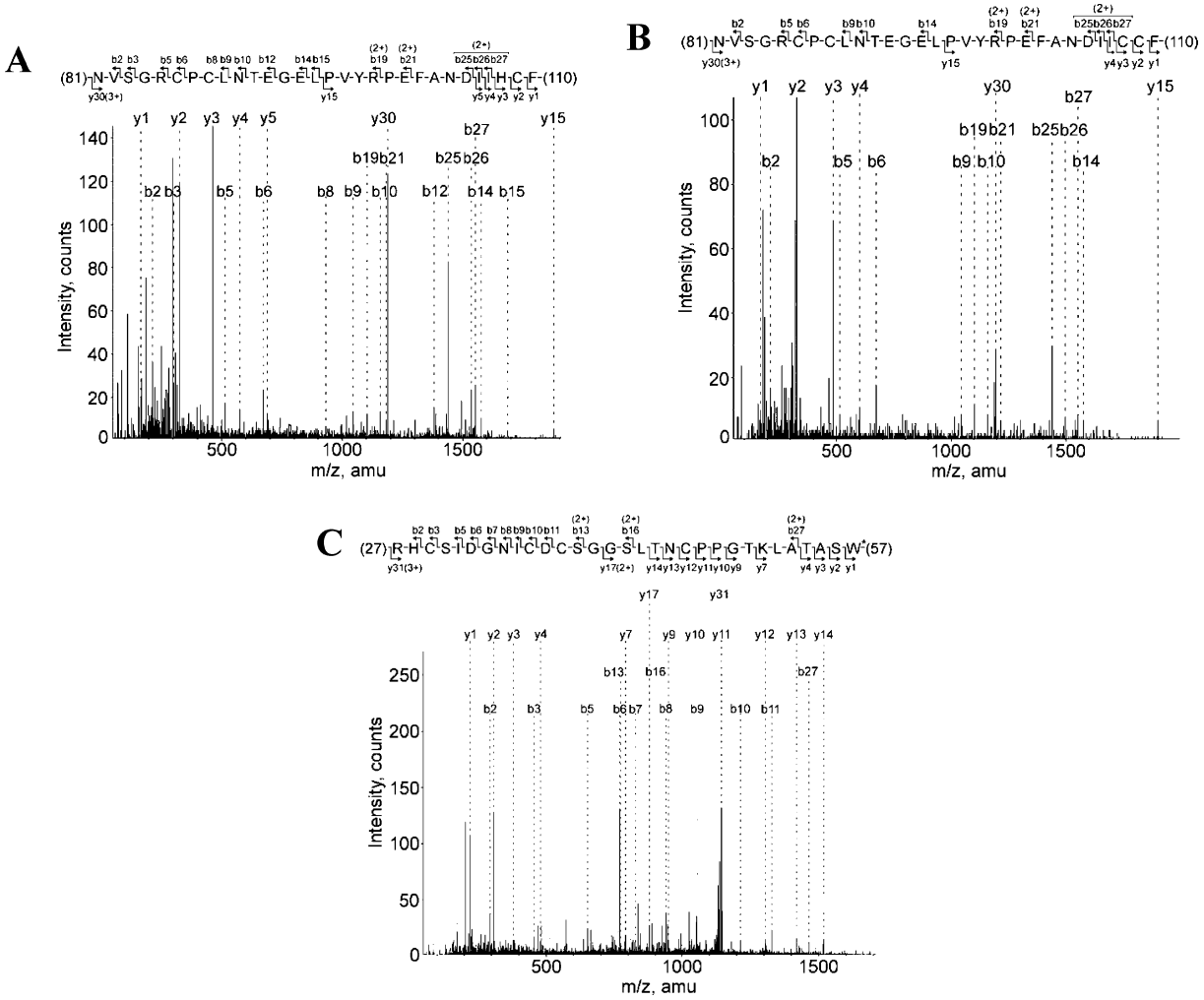

FIGURE 6: MS/MS spectra from fragmented proteolyzed peptides of βW108H and βW108C MADH mutants obtained by ESI-QTOF. Cysteine residues were protected from oxidation, and their masses include the addition of carboxamidomethyl. Product ions that were observed in the spectrum only as a multicharged species have the charge indicated in parentheses. Tolerance for *m*/*z* peak matches with product ions was set at ±150 ppm, and only b and y ions with intensities greater than 2% have been reported. Panel A shows the MS/MS spectrum of the triply charged ion of peptide βAsn^{81}−βPhe^{110} from βW108H MADH at *m*/*z* 1188.9 generated by chymotrypsin cleavage. The *m*/*z* peaks for product ions y1, y2, and y3 confirm the βTrp^{108} to histidine amino acid change in this mutant. Panel B shows the MS/MS spectrum of the triply charged ion of peptide βAsn^{81}−βPhe^{110} from βW108C MADH at *m*/*z* 1196.8 generated by chymotrypsin cleavage. The *m*/*z* peaks for product ions y1, y2, and y3 confirm the βTrp^{108} to cysteine amino acid change in this mutant. Panel C shows the MS/MS spectrum of the triply charged ion of peptide βArg^{27}−βTrp^{57} from βW108H MADH at *m*/*z* 1136.8 generated by chymotrypsin cleavage. The position of βTrp^{57}, the residue that becomes the quinone, is indicated by W* in the sequence. The *m*/*z* peaks for product ions y1, y2, y3, y4, y7, y9, y10, y11, y12, y13, y14, and y17 only matched the spectrum when a hydroxyl was added to the mass of βTrp^{57} in place of a hydrogen.

of 1.5 M guanidine-HCl and that under these conditions a single proteolysis step using either chymotrypsin or trypsin could completely cleave the β subunit of MADH into small peptides, as assessed by MALDI-TOF mass spectral analysis. The detailed protocol is described under Experimental Procedures. As an extension of the previous study and for comparison with the results obtained with H35V/MADH and H205V/MADH, this protocol was also applied to βW108H and βW108C MADH.

Chymotrypsin digests of βW108H and βW108C MADH, followed by mass spectrometry analysis and MS/MS fragmentation, revealed in each the presence of the un-cross-linked residue β^{108}-containing peptide. In the case of βW108H, there was a histidine at position β108, and for βW108C, there was a carboxamidomethyl-modified cysteine at position β108 (Figure 6A,B). For W108H, the βTrp^{57}-containing peptide was also discernible in the chymotrypsin digest, and MS/MS fragmentation and sequencing demonstrated that an extra oxygen in the form of a hydroxyl was present on βTrp^{57} in this sample as well (Figure 6C). These data demonstrate conclusively that the cross-link between residues βTrp^{57} and βTrp^{108} is absent not only in H35V/MADH and H205V/MADH but also in βW108H and βW108C MADH. For H35V/MADH, H205V/MADH, and βW108H MADH, the single posttranslationally incorporated oxygen is present in the form of a hydroxyl group on βTrp^{57}, and this is presumably also the case for βW108C MADH. No *m*/*z* peaks corresponding to un-cross-linked peptides containing either βTrp^{57} or βTrp^{108} were present in proteolytic digests of wtMADH.

DISCUSSION

Earlier studies of *P. denitrificans* cells in which the *mauG* gene was disrupted indicated a role for MauG in maturation of TTQ (*1*). Specifically, it was shown that although near wild-type levels of the MADH β subunit were expressed in

a *mauG* deletion strain of cells, the cells were unable to grow on methylamine as the sole carbon source and cell extracts were lacking in MADH activity. Furthermore, extracts of these cells did not exhibit the characteristic fluorescence associated with the reduced form of TTQ upon addition of methylamine (*1*). Although the structure of MauG is not known, the identity of the cysteine residues that are involved in covalent heme attachment and the histidine residues that provide a proximal ligand for each heme may be inferred from the amino acid sequence. Our intent in generating the H35V and H205V *mauG* mutations in the heterologous MADH expression system was to selectively disrupt each heme of MauG. Analysis of the effects of these mutations has allowed us to define roles for MauG in TTQ biogenesis. The results described in this study clearly indicate that MauG is involved in initiating both the cross-link formation between βTrp^{57} and βTrp^{108} and the incorporation of the second oxygen into βTrp^{57} to form the mature TTQ cofactor. The MADH expressed in the background of the *mauG* mutations is predominantly monoxygenated through the addition of a hydroxyl group to βTrp^{57}. These results are consistent with properties of the recently characterized MauG protein, which are more similar to those of an oxygenase than a peroxidase despite sequence similarity to diheme cytochrome *c* peroxidases (*16*).

In this study of the role of MauG in MADH biosynthesis, the results are essentially identical whether His^{35} or His^{205} is mutated, suggesting that both hemes contribute equally to activity. A caveat to this, however, is that attempts to express the H35V and H205V MauG mutant proteins in *P. denitrificans* cells, which were successfully used to express recombinant wild-type MauG (*16*), resulted in undetectable levels of either mutant protein (data not shown). This suggests that the mutants are not correctly synthesized or are extremely unstable after synthesis in *P. denitrificans*. This is likely also true in the *R. sphaeroides* cells of the heterologous expression system used to produce the H35V/MADH and H205V/MADH proteins. Thus, the similar results obtained for H35V/MADH and H205V/MADH may be the result of a general disruption of MauG in each case. Therefore, the results of this study clearly define the role of MauG in TTQ biogenesis. Further site-directed mutagenesis studies of *mauG* are planned to clearly define the roles of each heme of MauG in TTQ biogenesis.

A small and variable percentage of the MADH expressed in the presence of the *mauG* mutations has a mass that would be consistent with a fully synthesized TTQ in the β subunit (Figure 3). This suggests that some MauG activity may be present in the H35V and H205V mutants, albeit at a much lower level. Alternatively, this activity may be due to another enzyme present in the *R. sphaeroides* expression system that is able to nonspecifically catalyze these reactions but relatively inefficiently. Subpopulations of H35V/MADH and H205V/MADH also run as the holo enzyme on native PAGE and stain positively for MADH activity (Figure 2B,C) suggesting that this corresponds to the protein containing the small fraction of fully synthesized TTQ. The majority of the protein runs as the separate subunits on native PAGE, and the separated subunits do not stain for activity. The loss of heterotetramer stability in partially synthesized TTQ was also observed in our previous characterization of βW108H and βW108C MADH mutants (*12*; Figure 2B,C). In each case, higher activity always corresponds to a higher content of fully biosynthesized MADH in mass spectrometry studies and a larger amount of active heterotetramer in native PAGE, confirming our interpretation of the data.

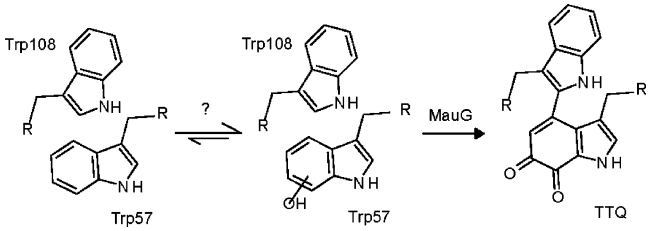

FIGURE 7: Proposed scheme of TTQ biosynthesis.

Our previous work on MADH mutants of βTrp^{108} has shown that the incorporation of the second oxygen into βTrp^{57} and the cross-linking of βTrp^{108} and βTrp^{57} were strongly coupled or occurred concomitantly. This result is confirmed in this study. Furthermore, it is shown that the conversion of the hydroxyl group on βTrp^{57} to a carbonyl is also coupled or concomitant chemistry in this reaction. Depending on the final mechanism of TTQ biogenesis, this conversion could either be a keto−enol tautomerization or part of an oxidative event. This study indicates an enzymatic role for MauG in this set of chemistries. The relatively weaker $\alpha\beta$ subunit interactions in the partially processed monohydroxylated forms of MADH are consistent with further TTQ biogenesis steps being catalyzed by one or more enzymes, one of which is MauG. The enzymes would require access to the TTQ tryptophans, which would not be possible if a stable heterotetramer had been formed at this stage. In the βTrp^{108} mutant study, we suggested that the absence of the cross-link would enable the loop (βLeu^{90}−βTrp^{108}) that forms the major part of the $\alpha\beta$ interface to be more flexible and destabilize the native oligomer, thus creating an enzyme recognition site. The βTrp^{108} mutants demonstrate that the β^{108} residue helps define the enzyme binding site and is not as efficiently recognized and chemically competent when mutated.

Present in H35V/MADH and H205V/MADH samples is a very minor species corresponding to a β subunit with no additional oxygens, which is never observed in preparations of wtMADH isolated in the same heterologous expression system. The mechanism of the initial monohydroxylase reaction is not known; however, if it is not very favorable, then without MauG to catalyze the subsequent step in biogenesis some of the unoxygenated substrate will remain present. In the presence of MauG, the monohydroxylated MADH β subunit, which serves as its substrate, will be removed by reaction, and as this occurs, the remaining unoxygenated form will be depleted to maintain equilibrium (Figure 7). Thus, even though MauG may not catalyze the initial hydroxylation, its activity will indirectly influence the amount of incomplete MADH with no additional oxygens via this equilibrium effect. Previous analysis of βW108H and βW108C MADH mutants also revealed a minor species corresponding to a β subunit with no additional oxygens (*12*). By the same logic, these mutations that decrease completion of TTQ biogenesis would also result in the presence of this species due to the equilibrium with the monohydroxylated intermediate.

In this study, we have demonstrated that MauG is involved in the completion of biogenesis through the formation of the

TTQ cross-link, the conversion of a single hydroxyl on βTrp^{57} to a carbonyl, and the incorporation of the second oxygen into the TTQ ring, not necessarily in that order. We have also demonstrated that all these chemistries are strongly coupled or occur concomitantly, because one modification was not observed without the others. While details of the mechanism of TTQ biogenesis remain to be elucidated, these results support the previous characterization of MauG as a di-*c*-type heme protein with oxygenase-like characteristics, which would be a novel reactivity for this class of enzymes (*16*). Efforts to separate the monohydroxylated H35V/MADH and H205V/MADH β subunits for crystallization trials are currently underway to identify the atomic site on βTrp^{57} of the initial hydroxylation, and in vitro studies with MauG and H35V/MADH and H205V/MADH are planned to precisely define the catalytic role of MauG in TTQ biogenesis.

ACKNOWLEDGMENT

We thank Yu Tang, LeeAnn Higgins, and Tom Krick for technical support.

REFERENCES

1. van der Palen, C. J., Slotboom, D. J., Jongejan, L., Reijnders, W. N., Harms, N., Duine, J. A., and van Spanning, R. J. (1995) Mutational analysis of *mau* genes involved in methylamine metabolism in *Paracoccus denitrificans*, *Eur. J. Biochem. 230*, 860−871.
2. Davidson, V. L. (2001) Pyrroloquinoline quinone (PQQ) from methanol dehydrogenase and tryptophan tryptophylquinone (TTQ) from methylamine dehydrogenase, *Adv. Protein Chem. 58*, 95−140.
3. Husain, M., and Davidson, V. L. (1985) An inducible periplasmic blue copper protein from *Paracoccus denitrificans*. Purification, properties, and physiological role, *J. Biol. Chem. 260*, 14626−14629.
4. Davidson, V. L., and Kumar, M. A. (1989) Cytochrome *c*-550 mediates electron transfer from inducible periplasmic *c*-type cytochromes to the cytoplasmic membrane of *Paracoccus denitrificans*, *FEBS Lett. 245*, 271−273.
5. Husain, M., and Davidson, V. L. (1986) Characterization of two inducible periplasmic *c*-type cytochromes from *Paracoccus denitrificans*, *J. Biol. Chem. 261*, 8577−8580.
6. Schwartz, B., and Klinman, J. P. (2001) Mechanisms of biosynthesis of protein-derived redox cofactors, *Vitam. Horm. 61*, 219−239.
7. Okeley, N. M., and van der Donk, W. A. (2000) Novel cofactors via posttranslational modifications of enzyme active sites, *Chem. Biol. 7*, R159−171.
8. Cai, D., and Klinman, J. P. (1994) Evidence of a self-catalytic mechanism of 2,4,5-trihydroxyphenylalanine quinone biogenesis in yeast copper amine oxidase, *J. Biol. Chem. 269*, 32039−32042.
9. Ruggiero, C. E., Smith, J. A., Tanizawa, K., and Dooley, D. M. (1997) Mechanistic studies of topa quinone biogenesis in phenylethylamine oxidase, *Biochemistry 36*, 1953−1959.
10. Matsuzaki, R., Fukui, T., Sato, H., Ozaki, Y., and Tanizawa, K. (1994) Generation of the topa quinone cofactor in bacterial monoamine oxidase by cupric ion-dependent autooxidation of a specific tyrosyl residue, *FEBS Lett. 351*, 360−364.
11. McIntire, W. S., Wemmer, D. E., Chistoserdov, A., and Lidstrom, M. E. (1991) A new cofactor in a prokaryotic enzyme: tryptophan tryptophylquinone as the redox prosthetic group in methylamine dehydrogenase, *Science 252*, 817−824.
12. Pearson, A. R., Jones, L. H., Higgins, L., Ashcroft, A. E., Wilmot, C. M., and Davidson, V. L. (2003) Understanding quinone cofactor biogenesis in methylamine dehydrogenase through novel cofactor generation, *Biochemistry 42*, 3224−3230.
13. Chistoserdov, A. Y., Boyd, J., Mathews, F. S., and Lidstrom, M. E. (1992) The genetic organization of the *mau* gene cluster of the facultative autotroph *Paracoccus denitrificans*, *Biochem. Biophys. Res. Commun. 184*, 1181−1189.
14. Chistoserdov, A. Y., Chistoserdova, L. V., McIntire, W. S., and Lidstrom, M. E. (1994) Genetic organization of the *mau* gene cluster in *Methylobacterium extorquens* AM1: complete nucleotide sequence and generation and characteristics of *mau* mutants, *J. Bacteriol. 176*, 4052−4065.
15. van der Palen, C. J., Reijnders, W. N., de Vries, S., Duine, J. A., and van Spanning, R. J. (1997) MauE and MauD proteins are essential in methylamine metabolism of *Paracoccus denitrificans*, *Antonie van Leeuwenhoek 72*, 219−228.
16. Wang, Y., Graichen, M. E., Liu, A., Pearson, A. R., Wilmot, C. M., and Davidson, V. L. (2003) MauG, a novel diheme protein required for tryptophan tryptophylquinone biogenesis, *Biochemistry 42*, 7318−7325.
17. Graichen, M. E., Jones, L. H., Sharma, B. V., van Spanning, R. J., Hosler, J. P., and Davidson, V. L. (1999) Heterologous expression of correctly assembled methylamine dehydrogenase in *Rhodobacter sphaeroides*, *J. Bacteriol. 181*, 4216−4222.
18. Zhu, Z., Jones, L. H., Graichen, M. E., and Davidson, V. L. (2000) Molecular basis for complex formation between methylamine dehydrogenase and amicyanin revealed by inverse mutagenesis of an interprotein salt bridge, *Biochemistry 39*, 8830−8836.
19. Mather, M. W., McReynolds, L. M., and Yu, C. A. (1995) An enhanced broad-host-range vector for gram-negative bacteria: avoiding tetracycline phototoxicity during the growth of photosynthetic bacteria, *Gene 156*, 85−88.
20. Davidson, V. L. (1990) Methylamine dehydrogenases from methylotrophic bacteria, *Methods Enzymol. 188*, 241−246.
21. Davidson, V. L., and Jones, L. H. (1992) Cofactor-directed inactivation by nucleophilic amines of the quinoprotein methylamine dehydrogenase from *Paracoccus denitrificans*, *Biochim. Biophys. Acta 1121*, 104−110.
22. Davidson, V. L., and Sun, D. (2002) Lysozyme-osmotic shock methods for localization of periplasmic redox proteins in bacteria, *Methods Enzymol. 353*, 121−130.
23. Simon, R., Priefer, U., and Puhler, A. (1983) A broad host range mobilization system for in vivo genetic engineering: transposon mutagenesis in gram negative bacteria., *Bio/Technology 1*, 784−791.

BI049863L